

Evaluation of Methods That Locate the Center of the Ankle for Computer-assisted Total Knee Arthroplasty

Robert A. Siston, MS[‡]; Aaron C. Daub, MS*[‡]; Nicholas J. Giori, MD, PhD*[‡][‡];
Stuart B. Goodman, MD, PhD*[‡]; and Scott L. Delp, PhD*[‡][§]*

Accurate alignment of the mechanical axis of the limb is important to the success of a total knee arthroplasty. Although computer-assisted navigation systems can align implants more accurately than traditional mechanical guides, the ideal technique to determine the distal end point of the mechanical axis, the center of the ankle, is unknown. In this study, we evaluated the accuracy, precision, objectivity, and speed of five anatomic methods and two kinematic methods for estimating the ankle center in 11 healthy subjects. Magnetic resonance images were used to characterize the shape of the ankle and establish the true ankle center. The most accurate and precise anatomic method was establishing the midpoint of the most medial and most lateral aspects of the malleoli (4.5 ± 4.1 mm lateral error; 2.7 ± 4.5 mm posterior error). A biaxial model of the ankle (2.0 ± 6.4 mm medial error; 0.3 ± 7.6 mm anterior error) was the most accurate kinematic method. Establishing the midpoint of the most medial and most lateral aspects of the malleoli was an accurate, precise, objective, and fast method for establishing the center of the ankle.

The success of a total knee arthroplasty (TKA) depends, in part, on accurate alignment of implants. Errors in alignment with respect to the mechanical axis of the limb can

lead to suboptimal postoperative outcomes and may contribute to implant loosening.^{9,14} The position and slope of the tibial component also can affect component wear²² and tibiofemoral kinematics.^{5,7,15} Computer-assisted surgical navigation systems^{4,19} have been developed to align implants more accurately than traditional mechanical guides, and surgeons using these systems have reported more accurate alignment of implants than with traditional mechanical alignment tools.^{3,10,17,18}

Navigation systems must accurately establish the mechanical axis of the limb, and, therefore, must accurately locate the ankle center, the distal end point of the mechanical axis. Developers of navigation systems have proposed several methods to establish the ankle center. These methods can be grouped into two categories: anatomic methods and kinematic methods. Anatomic methods require the surgeon to digitize certain anatomic landmarks during the operation. Inkpen and Hodgson examined the ability to locate the midpoint of the transmalleolar axis.⁸ Nofrini et al examined the ability to locate the midpoint between the most distal apexes of the malleoli and to project the digitized tendon of the tibialis anterior onto a transmalleolar axis.¹³ Krackow et al used a digitized vector that represented the surgeon's best estimate of the center of the ankle in the frontal plane.¹¹ Kinematic (motion-based) algorithms require the surgeon to displace the foot and ankle through a prescribed motion, and then an algorithm estimates the center of the ankle. Leitner et al treated the ankle as a ball-and-socket joint,¹² and van den Bogert proposed a biaxial model of the ankle.²¹

Computer-assisted navigation systems for TKA should establish the position of the ankle center with less than 6 mm error, as this corresponds to approximately 1° component alignment error. However, the best method for locating the ankle center to this level of accuracy is unknown. Nofrini et al evaluated a sample of anatomic algorithms and used computed tomography (CT) scans to establish a gold standard, but they did not investigate kinematic algorithms.¹³ Inkpen and Hodgson suggested that

Received: August 27, 2004

Revised: January 29, 2005; April 4, 2005

Accepted: April 27, 2005

From the *Mechanical Engineering Department; and the †Department of Orthopaedic Surgery, Stanford University, Stanford, CA; the ‡Department of Orthopaedic Surgery, Palo Alto Veterans Affairs Health Care System, Palo Alto, CA; and the §Bioengineering Department, Stanford University, Stanford, CA.

One of the authors (RS) has received funding from the participating faculty and a Whitaker Foundation Pre-Doctoral Fellowship.

Each author certifies that his or her institution has approved the human protocol for this investigation and that all investigations were conducted in conformity with ethical principles of research, and that informed consent was obtained.

Correspondence to: Scott L. Delp, PhD, Department of Bioengineering, S-321 James H. Clark Center, 318 Campus Drive, Stanford, CA 94305-5450. Phone: 650-723-1230; Fax: 650-723-8544; E-mail: delp@stanford.edu.

DOI: 10.1097/01.blo.0000170873.88306.56

anatomic methods provide a more repeatable determination of the ankle center than a ball-and-socket model of the ankle.⁸ No study has yet provided a comprehensive evaluation of methods that locate the center of the ankle for computer-assisted TKA.

The purpose of this study was to evaluate the accuracy, precision, objectivity, and speed of seven methods that estimate the center of the ankle and relate the results to the underlying bony anatomy measured via magnetic resonance (MR) images.

MATERIALS AND METHODS

We evaluated seven methods for determining the ankle center with a series of experiments involving 11 healthy subjects. Informed consent was obtained from all participants in accordance with Stanford University's Institutional Review Board. Data were collected using two Traxtal PassTrax reference frames (Traxtal Technologies Inc., Toronto, Ontario, Canada), a passive stylus, and a Polaris optical tracking system that sampled the position and orientation of the reference frames and the stylus at 30 Hz (Northern Digital Inc., Waterloo, Ontario, Canada). At a distance of 1.0–2.4 m, this optical system is accurate to within 2 mm for the measurement volume used in this study (Traxtal Technologies Inc.). The passive reference frames were attached to the volunteers' tibia and calcaneus with metal brackets and Velcro™ straps (McMaster-Carr, Los Angeles, CA) (Fig 1).

We investigated five different anatomic methods and two kinematic methods. One operator (RAS) made all of the measurements using a procedure that was agreed on by all authors. Each anatomic method (Fig 2) was repeated 10 times to characterize the differences between trials on the same subject. For the center estimate method, the operator first established a transmalleolar axis with the points used in the extremes midpoint method and then digitized his best estimate of the center of the ankle in the frontal plane. This point then was projected onto the transmalleolar axis to locate the ankle center. Similarly, with the TA projection method, the operator digitized the tendon of the tibi-

alis anterior; this point then was projected onto the transmalleolar axis, which was established with the points used in the extremes midpoint method, to estimate the ankle center. With the sphere-fit method, a sphere was fit⁶ to five points that were digitized on each malleolus (Fig 2), and the midpoint of the center of the two spheres was used as the center of the ankle. With all anatomic methods, the operator pulled his hands away and looked away from the subject's ankle after each trial to ensure that the same points were not retargeted in successive trials. Additionally, the operator avoided making skin impressions with the optical stylus, which would allow him to retarget the same point.

For the two kinematic methods (Fig 3), a passive reference frame was attached to each subject's calcaneus with a metal bracket and elastic strap (Fig 1B). For the ball-and-socket method, we circumducted the foot through the passive range of motion (ROM) of the ankle and used a least-squares optimization⁶ to fit a sphere to the set of points defined by the motion of the calcaneus relative to the tibia. For the biaxial model, we manipulated the foot through the eight motion patterns used by van den Bogert et al.²¹ These motions were: (1) pure plantar-dorsiflexion, (2) plantar-dorsiflexion with the foot everted, (3) plantar-dorsiflexion with the foot inverted, (4) pure pronation-supination, (5) pronation-supination with the foot dorsiflexed, (6) pronation-supination with the foot semiplantar flexed, (7) pronation-supination with the foot in a full-plantar flexed position, and (8) a full circumduction movement at the extreme ROM for the ankle. We then used an adaptation of kinematic dyad theory (Appendix) to establish a biaxial model of the ankle that consisted of two revolute joints representing the talocrural and subtalar axes. The intersection of the talocrural and subtalar axes, when projected onto the transverse plane of the tibia²³ then was taken to be the center of the ankle.

We used MR images to characterize the shape of the ankle and to establish the true ankle center. We used vitamin E capsules as fiducial markers to relate the data collected during the trial to the MR images. A neoprene cuff with vitamin E capsules was strapped to the subject's distal tibia (Fig 1A), and the operator digitized these markers. The operator then removed the

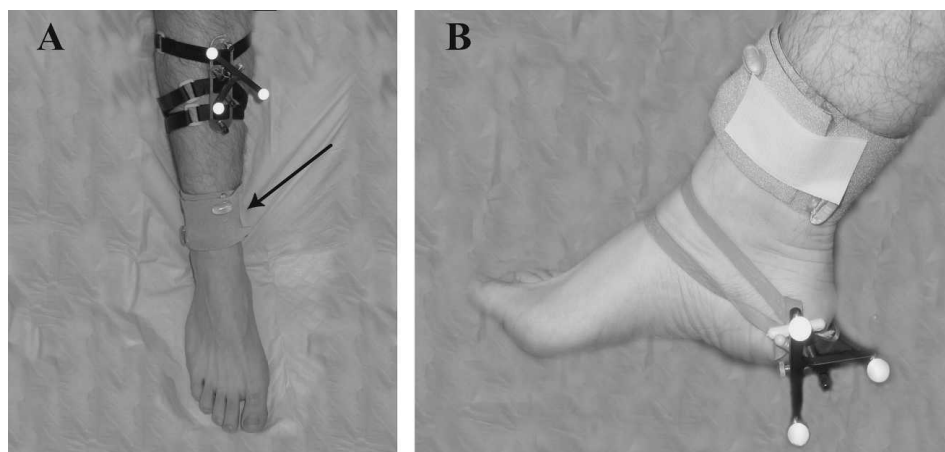


Fig 1A–B. (A) Passive reference frames were attached to subjects with a metal bracket and straps. A neoprene cuff with vitamin E tablets (arrow) was used to register the experimental data to the MR images. (B) A reference frame is attached to a subject's calcaneus to record motion data for the kinematic methods.

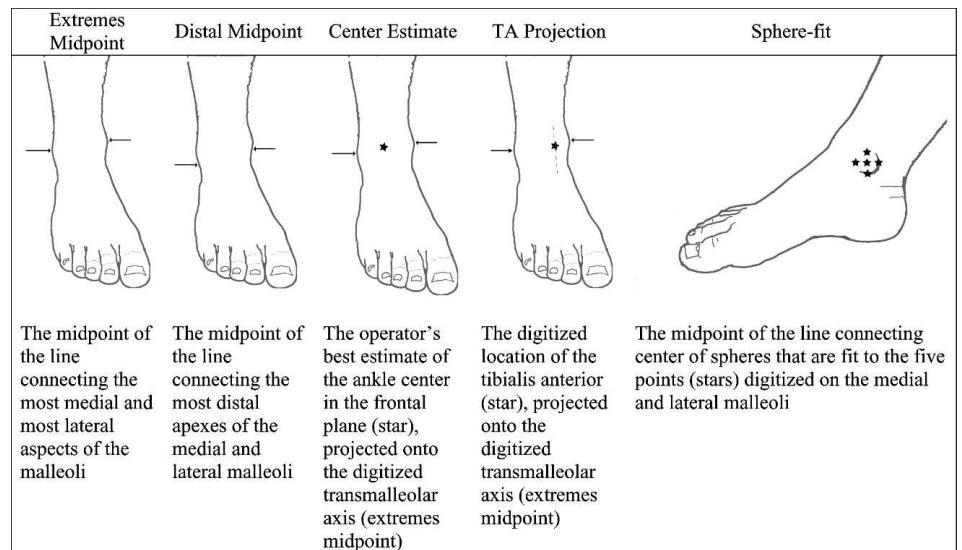


Fig 2. The five anatomic methods used to estimate the ankle center are illustrated.

passive reference frames from the subject's leg. The subject's ankle, foot, and distal-third of the tibia then were scanned with a GE 1.5T Signa magnet (General Electric Healthcare Technologies, Waukesha, WI) using a three-dimensional FGRE sequence (TR = 8.1 ms, TE = 3.2 ms, 30° flip angle) with a 24-cm FOV, 0.9375-mm in-plane resolution, and 1-mm slice thickness.

We segmented the images to identify the fiducial markers, the most medial and most lateral aspects of the malleoli, the distal apices of the malleoli, and the distal articulating surface of the tibia. The location of the fiducial markers, the most medial and lateral aspects of the malleoli, and the distal apices of the malleoli were used to register the MR images to the experimental data with an iterative closest point algorithm.¹

We defined the distal end point of the tibial mechanical axis as the intersection of two diagonal lines that were drawn from the corners of the weightbearing distal articulating surface of the tibia²³; this point served as the true ankle center for our experiments. This definition of the ankle center was an objective method of defining the distal end point of the mechanical axis that could be located on the images in the frontal and sagittal planes.

We defined the error associated with each method as the distance between our true ankle center and the ankle center calculated from the various methods. We did all calculations for the methods on a Dell PC (Pentium 4, 2GHz; Round Rock, TX). We assessed the precision of each method by investigating its standard deviation, and we used the Bartlett test to evaluate homogeneity of variance among the methods. After identifying unequal variances of the techniques, we used the Kruskal-Wallis test (a nonparametric test analogous to an analysis of variance (ANOVA), but one that can compensate for unequal variances between techniques) to assess accuracy and identify statistically significant differences in the mean errors of the methods, and the Tukey-Kramer method was used to further investigate significant results. The level of statistical significance was set at $\alpha = 0.05$.

RESULTS

Four anatomic methods (extremes midpoint, distal midpoint, center estimate, and sphere fit) and one kinematic

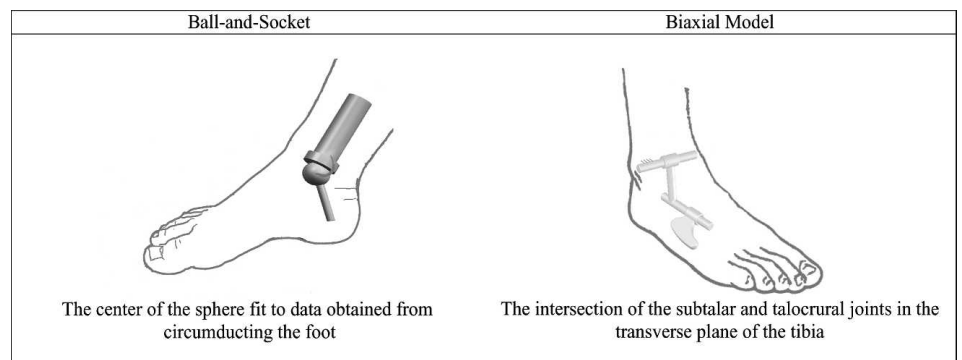


Fig 3. The two kinematic methods used to estimate the ankle center are shown.

method (biaxial model) had median errors less than 6 mm in the frontal plane (Fig 4). Among these five methods, the sphere fit had a larger mean error ($p < 0.05$) than the others. The fifth anatomic method, TA projection, was medially biased by an average of 16.5 ± 4.6 mm. The biaxial model was the most accurate kinematic method (2.0 ± 6.4 mm medial error), whereas the ball-and-socket method had the largest standard deviation of the mean error of all techniques in the frontal plane with a 16.2 ± 28.7 mm lateral error. As determined by the standard deviation of the mean error, the extremes midpoint (4.5 ± 4.1 mm lateral error), distal midpoint (3.7 ± 4.5 mm lateral error), and TA projection methods were the most precise methods in the frontal plane.

All of the methods except the ball-and-socket had median errors less than 6 mm in the sagittal plane (Fig 5). The biaxial model had the smallest mean error (0.3 ± 7.6 mm anterior error), but there was no significant difference between it and the center estimate and TA projection methods. The TA projection was biased anteriorly (mean 1.7 ± 5.7 mm anterior error), whereas the center estimate was biased posteriorly (1.5 ± 4.1 mm posterior error). There was no significant difference between the mean errors for the center estimate and extremes midpoint (2.7 ± 4.5 mm posterior error) and sphere fit (2.6 ± 4.6 mm posterior error) methods. The ball-and-socket had the largest mean errors in the sagittal plane (7.1 ± 13.6 mm posterior error).

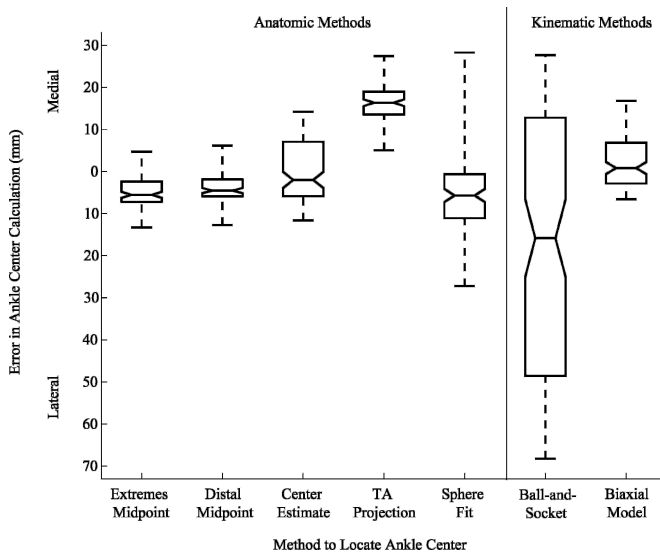


Fig 4. The frontal plane errors in the estimation of the ankle center for five anatomic and two kinematic methods are shown. The horizontal lines across each box represent the median error. The box edges represent the upper and lower quartiles of the data, and the error bars represent the total range of the data.

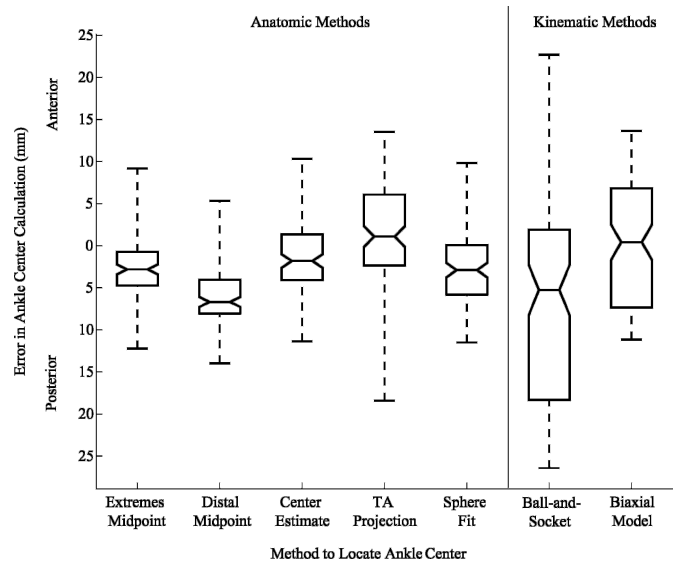


Fig 5. The sagittal plane errors in the estimation of the ankle center for five anatomic and two kinematic techniques are shown. The horizontal lines across each box represent the median error. The box edges represent the upper and lower quartiles of the data, and the error bars represent the total range of the data.

The four most precise methods were the extremes midpoint, distal midpoint (5.8 ± 3.9 mm posterior error), center estimate, and sphere fit.

We implemented all but one of the anatomic methods in less than approximately 10 seconds. The sphere fit method required approximately 30 seconds to identify all points on the malleoli. Using the circumduction pattern for the ball-and-socket method required approximately 10 seconds, and an additional minute of computational time was needed to locate the ankle center. We acquired the eight motion patterns for the biaxial model in approximately 2 minutes, but approximately 3 minutes of additional computational time was needed to do all of the calculations associated with this method.

DISCUSSION

We examined the differences in performance among various methods of determining the ankle center. Nofrini et al¹³ reported similar results to ours with the extremes midpoint and distal midpoint methods (mean errors of 0.9° and 1.1° , respectively, or approximately 6 mm), but also reported the TA projection method to be slightly less accurate (mean error of $3.5^\circ \pm 0.6^\circ$, or approximately 21 mm) than what we determined. Inkpen and Hodgson⁸ implemented the ball-and-socket method with a tracker strapped to the foot and reported errors that were 4.6 mm lateral and

7.0 mm anterior to an ankle center obtained with the extremes midpoint method. Although our measurement error with the ball-and-socket method is larger, we concur with their suggestion that anatomic methods are more repeatable than this kinematic model of the ankle.

Our study has some limitations. We did not attach the reference frame to the tibia with bone screws, and this nonrigid attachment may have permitted a small amount of reference frame motion, inducing error into the measurements. Also, we did not use draping around the foot and ankle, as draping may limit the operator's ability to palpate bony landmarks. We used MATLAB® (The MathWorks, Natick, MA) for our calculations, therefore, the amount of necessary computational time for the kinematic methods was longer in this experiment than what it would be for a program written in a precompiled language, such as C. Finally, we only used one operator in this study. Although our results are from an operator who is experienced with navigation systems and the relevant anatomy, future studies should compare and contrast the performance of different operators to fully investigate the subjectivity of these methods.

When choosing the method to determine the center of the ankle for computer-assisted TKA, the technique should meet certain criteria for accuracy (as evidenced by small mean errors), precision (small standard deviations of the mean error and small range of errors), objectivity (independent of operator bias), and speed of execution, as it is undesirable to use an accurate technique if it significantly increases the duration of an operation. Each of the methods in this study can be evaluated against those criteria. The ball-and-socket and the TA projection methods are too inaccurate to be considered ideal methods to locate the center of the ankle because implementing these techniques frequently would result in a greater than 1° angular alignment error in the frontal plane. The sphere fit method more accurately locates the ankle center, but its large standard deviation in the frontal plane and large measurement outliers indicate that this method is imprecise with the equipment used in our study. Our biaxial model is very accurate but requires the operator to manipulate the foot through eight motion patterns, and it takes several minutes for the optimization algorithm to compute the talocrural and subtalar axes. This additional time would unnecessarily increase the duration of an operation, because the biaxial model's performance was statistically equal to anatomic methods that can be implemented more quickly. Making the center estimate at the center of the ankle proved to be an accurate method, but the success of this subjective method is dependent on operator skill and the anatomy of the patient. This subjectivity is manifested in the lack of precision of this method in the frontal plane. Of the two remaining methods, establishing the distal midpoint was

statistically less accurate in the sagittal plane than establishing the extremes midpoint.

We found that establishing the midpoint of the most medial and most lateral aspects of the malleoli (the extremes midpoint method) is an accurate, precise, objective, and fast method for locating the center of the ankle. Our results show that this is an excellent method to establish the center of the ankle for computer-assisted TKA.

APPENDIX

The ankle can be modeled as a pair of revolute joints. The talocrural axis, located between the tibia and talus, serves as a plantar flexion-dorsiflexion axis. The subtalar axis, located between the talus and foot, serves as an inversion-eversion axis. We used kinematic dyad theory²⁰ to determine the location and the direction of these two revolute axes.

We recorded the position and orientation of the calcaneus reference frame with respect to the tibia reference frame while a subject's foot was in an initial, neutral position and while the operator manipulated a subject's foot through eight motion patterns. The kinematic data were low-pass filtered using a Butterworth filter with a 6 Hz cutoff frequency and were represented as a series of 4 × 4 homogeneous transformation matrices.

We used the transformation matrix expressing the calcaneus in the initial position (${}^{tibia}_1T$), and the transform matrices expressing the calcaneus in positions $j = 2 \dots n$ (${}^{tibia}_jT$) to obtain the kinematic screw displacements \hat{S}_{1j} .² As described by Bottema and Roth,² we located the direction of [${}^1\hat{s}_j$ (s_x, s_y, s_z)], rotation about (θ_{1j}), displacement along (t), and the location of [${}^1S_{0nj}$ (S_{0x}, S_{0y}, S_{0z})], \hat{S}_{1j} from the transformation matrices j_1T , which were found as follows:

$${}^j_1T = {}^{tibia}_1T * {}^{tibia}_jT = [{}^{tibia}_1T]^{-1} * {}^{tibia}_jT \quad (1)$$

The screw axes obtained from j_1T were expressed with respect to the initial position of the calcaneus. As filters to prevent screw axes that only represented translation, we excluded the axes that had less than 5° rotation. So that the final joint axes would be expressed with respect to the tibia, we transformed ${}^1\hat{s}_j$ and ${}^1S_{0nj}$ into the tibial reference frame with

$$\hat{S}_{1j} = {}^{tibia}_1R * {}^1\hat{s}_j \quad (2)$$

$$A_{1j} = {}^{tibia}_jT * {}^1S_{0nj} \quad (3)$$

Where ${}^{\text{tibia}}_1\mathbf{T}$ is defined previously and ${}^{\text{tibia}}_1\mathbf{R}$ is the 3×3 rotation matrix from ${}^{\text{tibia}}_1\mathbf{T}$.

We applied the equations from Tsai and Roth²⁰ who described a Revolute-Revolute dyad to solve for the location and direction of the talocrural and subtalar axes.

$$\tan \frac{\theta_{1j}}{2} = - \frac{\mathbf{F}_{1j} \cdot (\mathbf{S}_{1j} \times \mathbf{M}_{1j})}{(\mathbf{F}_{1j} \times \mathbf{S}_{1j}) \cdot (\mathbf{S}_{1j} \times \mathbf{M}_{1j})} \quad (4)$$

$$\begin{aligned} \frac{t_{1j}}{2} = & - \frac{\mathbf{S}_{1j} - (\mathbf{S}_{1j} \cdot \mathbf{M}_{1j}) \mathbf{M}_{1j}}{1 - (\mathbf{S}_{1j} \cdot \mathbf{M}_{1j})^2} \cdot (\mathbf{Q}_{1j} - \mathbf{A}_{1j}) \\ & + \frac{\mathbf{S}_{1j} - (\mathbf{S}_{1j} \cdot \mathbf{F}_{1j}) \mathbf{F}_{1j}}{1 - (\mathbf{S}_{1j} \cdot \mathbf{F}_{1j})^2} \cdot (\mathbf{G}_{1j} - \mathbf{A}_{1j}) \end{aligned} \quad (5)$$

$$\begin{aligned} \frac{u_{1j}}{2} = & \frac{\mathbf{M}_{1j} - (\mathbf{M}_{1j} \cdot \mathbf{F}_{1j}) \mathbf{F}_{1j}}{1 - (\mathbf{M}_{1j} \cdot \mathbf{F}_{1j})^2} \cdot (\mathbf{G}_{1j} - \mathbf{Q}_{1j}) \\ & - \frac{\mathbf{M}_{1j} - (\mathbf{M}_{1j} \cdot \mathbf{S}_{1j}) \mathbf{S}_{1j}}{1 - (\mathbf{M}_{1j} \cdot \mathbf{S}_{1j})^2} \cdot (\mathbf{A}_{1j} - \mathbf{Q}_{1j}) \end{aligned} \quad (6)$$

$$\begin{aligned} \frac{w_{1j}}{2} = & \frac{\mathbf{F}_{1j} - (\mathbf{F}_{1j} \cdot \mathbf{S}_{1j}) \mathbf{S}_{1j}}{1 - (\mathbf{F}_{1j} \cdot \mathbf{S}_{1j})^2} \cdot (\mathbf{A}_{1j} - \mathbf{G}_{1j}) \\ & - \frac{\mathbf{F}_{1j} - (\mathbf{F}_{1j} \cdot \mathbf{M}_{1j}) \mathbf{M}_{1j}}{1 - (\mathbf{F}_{1j} \cdot \mathbf{M}_{1j})^2} \cdot (\mathbf{Q}_{1j} - \mathbf{G}_{1j}) \end{aligned} \quad (7)$$

For this model of the ankle, $\widehat{\mathbf{S}}_{1j}$, describing the displacement from an initial position of the calcaneus to a subsequent position j , is fully delineated by the screw displacement about a moving joint axis, $\widehat{\mathbf{M}}_{1j}$ (the subtalar axis), and the screw displacement about a fixed joint axis, $\widehat{\mathbf{F}}_{1j}$ (the talocrural axis) (Fig 6). In this screw triangle,¹⁶ $\mathbf{F}(\mathbf{F}_{x1j}, \mathbf{F}_{y1j}, \mathbf{F}_{z1j})$ is a unit vector parallel to the initial, 1st, position of the $\widehat{\mathbf{F}}_{1j}$, and $\mathbf{G}(\mathbf{G}_{x1j}, \mathbf{G}_{y1j}, \mathbf{G}_{z1j})$ is an arbitrary point on $\widehat{\mathbf{F}}_{1j}$ that describes the location of this axis in the 1st position. Similarly, $\mathbf{M}(\mathbf{M}_{x1j}, \mathbf{M}_{y1j}, \mathbf{M}_{z1j})$ and $\mathbf{Q}(\mathbf{Q}_{x1j}, \mathbf{Q}_{y1j}, \mathbf{Q}_{z1j})$ describe the orientation and position of $\widehat{\mathbf{M}}_{1j}$; $\mathbf{S}(\mathbf{S}_{x1j}, \mathbf{S}_{y1j}, \mathbf{S}_{z1j})$ and $\mathbf{A}(\mathbf{A}_{x1j}, \mathbf{A}_{y1j}, \mathbf{A}_{z1j})$ describe the orientation and position of $\widehat{\mathbf{S}}_{1j}$; θ_{1j} and t_{1j} represent the rotational and translational displacements, respectively, about and along the screw $\widehat{\mathbf{S}}_{1j}$, and u_{1j} and w_{1j} represent the translational displacements along screws $\widehat{\mathbf{M}}_{1j}$ and $\widehat{\mathbf{F}}_{1j}$, respectively, from positions 1– j . Because there is no translational displacement along a pure revolute joint, $u_{1j} = w_{1j} = 0$. Finally, we defined screws $\widehat{\mathbf{F}}_{1j}$ and $\widehat{\mathbf{M}}_{1j}$ as unit vectors (Equations 8 and 9) and defined \mathbf{G}_{1j} and \mathbf{Q}_{1j} as the unique points along the joint-axes that are perpendicular to $\widehat{\mathbf{F}}_{1j}$ and $\widehat{\mathbf{M}}_{1j}$ (Equations 10 and 11):

$$\mathbf{F}_{1j} \cdot \mathbf{F}_{1j} = 1 \quad (8)$$

$$\mathbf{M}_{1j} \cdot \mathbf{M}_{1j} = 1 \quad (9)$$

$$\mathbf{F}_{1j} \cdot \mathbf{G}_{1j} = 0 \quad (10)$$

$$\mathbf{M}_{1j} \cdot \mathbf{Q}_{1j} = 0 \quad (11)$$

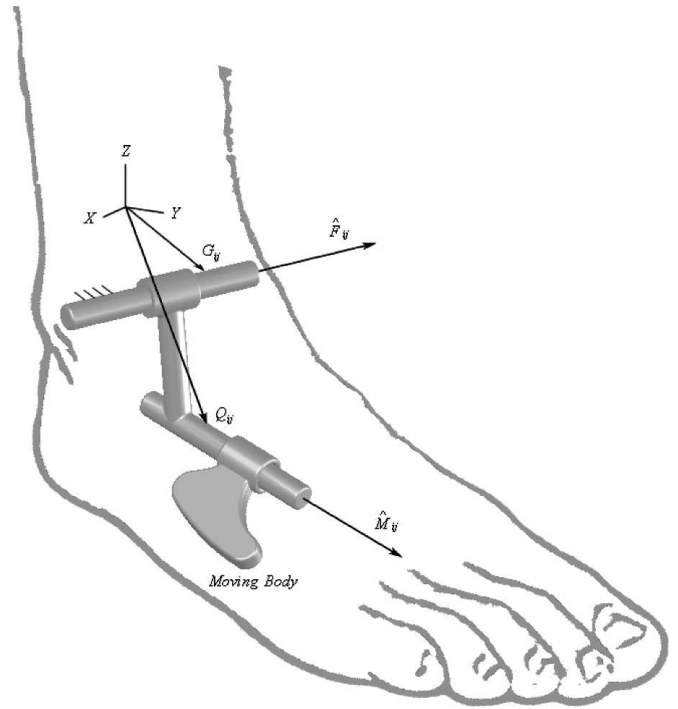


Fig 6. The location and orientation of the fixed and moving axes are identified with respect to the tibia reference frame in this biaxial ankle model.

For any set of three positions of the calcaneus, the parameters of \mathbf{F} , \mathbf{G} , \mathbf{M} , and \mathbf{Q} can be uniquely determined. However, because the ankle is not comprised of ideal revolute joints, these 12 parameters will not be identical for any arbitrary set of three positions of the calcaneus. By using data from the entire ROM of the ankle, the most representative parameters can be obtained, and finding a solution then involves an optimization procedure that minimizes the residuals of the constraining equations. For the k resultant screw axes, Equations 4–7 were written k times and Equations 8–11 were written once each. The average screw axes from two motion patterns, plantar-dorsiflexion and inversion-eversion, were taken as initial guesses for the direction and location of the fixed joint axis and the moving joint axis on a subject-specific basis. Appropriate bounds were placed on the optimization routine so that deviations greater than $\pm 30^\circ$ away from these initial guesses and solutions that yielded results physically located outside a subject's ankle were not possible. We did this nonlinear optimization with the `lsqnonlin` function from the MATLAB[®] Optimization Toolbox (The MathWorks, Natick, MA), which uses a large-scale algorithm that is a subspace trust region method based on the interior-reflective Newton method. The iterations of the optimization functions use the method of preconditioned conjugate gradients.

On converging to a solution, the parameters of F and G determined the best-fit talocrural joint, and the parameters M and Q determined the best-fit subtalar joint.

Acknowledgments

We thank Brian Hargreaves, Thor Besier, and Silvia Blemker for assistance.

References

1. Besl PJ, McKay ND: A method for registration of 3-D shapes. *IEEE Trans Pattern Anal Mach Intell* 14:239–256, 1992.
2. Bottema O, Roth B: *Theoretical Kinematics*. Mineola, Dover Publications 1990.
3. Chauhan SK, Scott RG, Bredahl W, Beaver RJ: Computer-assisted knee arthroplasty versus a conventional jig-based technique: A randomized, prospective trial. *J Bone Joint Surg* 86B:372–377, 2004.
4. Delp SL, Stulberg SD, Davies B, Picard F, Leitner F: Computer assisted knee replacement. *Clin Orthop* 354:49–56, 1998.
5. Dorr LD, Boiardo RA: Technical considerations in total knee arthroplasty. *Clin Orthop* 205:5–11, 1986.
6. Forbes AB: Least-squares best-fit geometric elements, National Physical Lab Report DITC 140/89. National Physical Laboratory, Teddington, UK April 1989.
7. Garg A, Walker PS: Prediction of total knee motion using a three-dimensional computer-graphics model. *J Biomech* 23:45–58, 1990.
8. Inkpen KB, Hodgson AJ: Accuracy and repeatability of joint center location in computer-assisted knee surgery. In Taylor C, Colchester A (eds). *Lecture Notes in Computer Science (Vol 1679): Medical Image Computing and Computer-Assisted Intervention—MICCAI '99: Second International Conference Cambridge, UK*. Heidelberg, Springer-Verlag 1072–1079, 1999.
9. Jeffery RS, Morris RW, Denham RA: Coronal alignment after total knee replacement. *J Bone Joint Surg* 73B:709–714, 1991.
10. Jenny JY, Boeri C: Computer-assisted implantation of a total knee arthroplasty: A case-controlled study in comparison with classical instrumentation. *Rev Chir Orthop Reparatrice Appar Mot* 87:645–652, 2001. [in French]
11. Krackow KA, Bayers-Thering M, Phillips MJ, Bayers-Thering M, Mihalko WM: A new technique for determining proper mechanical axis alignment during total knee arthroplasty: Progress toward computer-assisted TKA. *Orthopedics* 22:698–702, 1999.
12. Leitner F, Picard F, Minfelde R, et al: Computer assisted knee surgical total replacement. In Troccaz J, Grimson E, Mösges R (eds). *Lecture Notes in Computer Science (Vol 1205): CVRMed-MRCAS '97: First Joint Conference Computer Vision, Virtual Reality and Robotics in Medicine and Medical Robotics and Computer-Assisted Surgery Grenoble, France*. Heidelberg, Springer-Verlag 627–638, 1997.
13. Nofrini L, Slomczykowski M, Iacono F, Marcacci M: Evaluation of accuracy in ankle center location for tibial mechanical axis identification. *J Invest Surg* 17:23–29, 2004.
14. Oswald MH, Jakob RP, Schneider E, Hoogewoud HM: Radiological analysis of normal axial alignment of femur and tibia in view of total knee arthroplasty. *J Arthroplasty* 8:419–426, 1993.
15. Piazza SJ, Delp SL, Stulberg SD, Stern SH: Posterior tilting of the tibial component decreases femoral rollback in posterior-substituting knee replacement: A computer simulation study. *J Orthop Res* 16:264–270, 1998.
16. Roth B: On screw axes and other special lines associated with spatial displacements of a rigid body. *J Eng Industry* 89:102–110, 1967.
17. Saragaglia D, Picard F, Chaussard C, et al: Computer-assisted knee arthroplasty: Comparison with a conventional procedure. Results of 50 cases in a prospective randomized study. *Rev Chir Orthop Reparatrice Appar Mot* 87:18–28, 2001. [in French]
18. Stulberg SD: How accurate is current TKR instrumentation? *Clin Orthop* 416:177–184, 2003.
19. Stulberg SD, Loan P, Sarin V: Computer-assisted navigation in total knee replacement: Results of an initial experience in thirty-five patients. *J Bone Joint Surg* 84A(Suppl 2):90–98, 2002.
20. Tsai LW, Roth B: Design of dyads with helical, cylindrical, spherical, revolute and prismatic joints. *Mech Machine Theory* 7:85–102, 1972.
21. van den Bogert AJ, Smith GD, Nigg BM: In vivo determination of the anatomical axes of the ankle joint complex: An optimization approach. *J Biomech* 27:1477–1488, 1994.
22. Wasielewski RC, Galante JO, Leighty RM, et al: Wear patterns on retrieved polyethylene tibial inserts and their relationship to technical considerations during total knee arthroplasty. *Clin Orthop* 299:31–43, 1994.
23. Yoshioka Y, Siu DW, Scudamore RA, Cooke TD: Tibial anatomy and functional axes. *J Orthop Res* 7:132–137, 1989.